THE JOURNAL OF PHYSICAL CHEMISTRY B

Article

pubs.acs.org/JPCB

The Exciton Origin of the Visible Circular Dichroism Spectrum of Bacteriorhodopsin

Gennaro Pescitelli*,† and Robert W. Woody*,‡

†Dipartimento di Chimica e Chimica Industriale, Università degli Studi di Pisa, via Risorgimento 35, I-56126 Pisa, Italy

‡Department of Biochemistry and Molecular Biology, Colorado State University, Fort Collins, Colorado 80523, United States

Supporting Information

ABSTRACT: The visible CD spectrum of bacteriorhodpsin (bR) in purple membrane has a negative CD band at ∼600 nm and a positive band at ∼530 nm and has been variously interpreted as resulting from exciton coupling within the bR trimer, heterogeneity in protein conformation, or the presence of two distinct low-energy electronic transitions in bR. We have performed time-dependent density functional theory (TDDFT) calculations on the protonated Schiff base of retinal (retPSB) in bR to predict the intrinsic CD. The resulting spectroscopic parameters have been used to predict the long-wavelength CD spectrum of retPSB trimers. TDDFT, exciton theory, and classical polarizability (DeVoe) predict a strong negative couplet centered near 570 nm, with a magnitude in good agreement with experiment. Coupling of the retPSB chromophore with aromatic and peptide chromophores has been considered by means of perturbation theory and is responsible for the net positive CD of the 570 nm band. The visible CD spectrum of bR is dominated by exciton interactions.

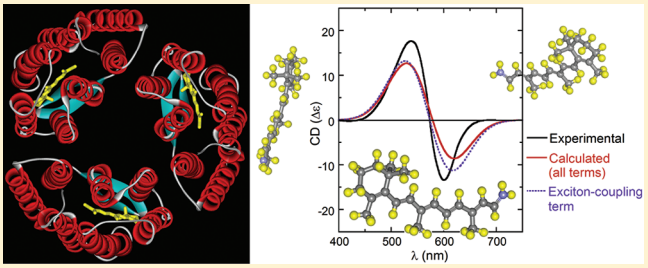

INTRODUCTION

The CD spectrum of purple membrane exhibits a strong negative band near 600 nm and a stronger positive band near 530 nm.[1,2] Such a pattern of closely spaced CD bands of opposite sign and roughly equal magnitudes is called a couplet[3,4] and is characterized by a sign which is that of the long-wavelength band. Thus, the CD of purple membrane has a negative couplet associated with the 570 nm absorption band. Early studies[1,2,5−7] recognized that three interpretations of this negative couplet are possible: exciton coupling within the bacteriorhodopsin (bR) trimers that make up purple membrane or a nonexciton origin from either protein heterogeneity or the existence of two distinct excited states of the retinal protonated Schiff base (retPSB). However, the exciton explanation was emphasized, and two studies aimed at deriving geometric information from the absorption and CD data were reported.[8,9] These analyses gave exciton splittings of ∼1500 and ∼600 cm^{-1}, respectively, from which interchromophoric distances of ∼10 and ∼16 Å, respectively, were inferred. The interchromophoric distance in the bR trimer is now known to be ∼31 Å, based upon X-ray diffraction.[10]

El-Sayed and co-workers[11−14] have argued against the exciton model of purple membrane CD and proposed that the CD couplet in bR results from protein heterogeneity, with two or more proteins having different conformations near the chromophore and giving rise to rotational strengths of opposite sign for the long-wavelength absorption band, or from two closely spaced electronic transitions in the retinal PSB. The arguments of El-Sayed and co-workers were countered by Cassim,[15] but the nonexciton interpretation was recently supported by studies of partially regenerated purple membrane.[16]

The purpose of the present work is to re-examine the origin of the CD couplet in purple membrane. We test the hypothesis that the source of the couplet is exciton coupling by performing exciton calculations of purple membrane CD and examining other sources of bR CD, such as twisting of the retinal PSB chromophore and coupling with aromatic and peptide chromophores. These calculations utilize the three-dimensional structure of bR from X-ray diffraction and time-dependent density functional theory (TDDFT) calculations on the retinal PSB chromophore. We find that the exciton interpretation of the bR CD spectrum is fully consistent with experiment and that the objections to the exciton mechanism raised by El-Sayed and co-workers[11−14] and by Kataoka et al.[17] and Karnaukhova et al.[16,18] are not valid.

METHODS

All calculation methods used are described in detail in the Supporting Information. The formulas contained in the Supporting Information are quoted in the following using the "S" prefix, e.g., eq S1.

Geometry. The starting geometries for all calculations have been obtained from two X-ray structures of bR, PDB codes

Special Issue: B: Harold A. Scheraga Festschrift

Received: December 16, 2011
Revised: February 3, 2012
Published: February 14, 2012

   dx.doi.org/10.1021/jp212166k | J. Phys. Chem. B 2012, 116, 6751−6763

1QM8 (resolution 2.2 Å)[19] and 1C3W (1.55 Å).[10] The input geometries for TDDFT and ZINDO calculations were generated by detaching the terminal N atom of the chromophore from the Lys residue and attaching two H atoms to produce a —CH=NH_2^+ terminal (see Chart 1). The

Chart 1

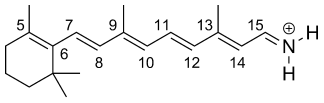

retPSB (bR pigment)

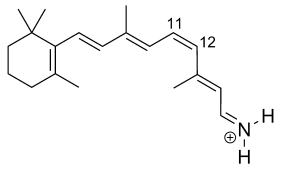

11*cis*-retPSB (Rh pigment)

remaining hydrogens were also added and preoptimized with MMFF. All hydrogen atoms of this all-*trans* PSB model (retPSB) were then optimized with DFT at the B3LYP/6-31G(d) level, while all heavy atoms were kept frozen. The atomic coordinates are given in Table S1 (Supporting Information). Although the limited resolution of X-ray structures may introduce some error in distances and angles if not further refined, at least the resolution of the 1C3W structure is good enough to ensure that the overall molecular shape is properly represented and, as a consequence, experimental CD spectra are correctly reproduced, when the X-ray geometry is used as input structure, as observed for several small organic compounds[20] and for rhodopsin.[21] MMFF and DFT geometry optimizations were run with Spartan'08.[22]

Quantum-Mechanical Calculations. Time-dependent density functional theory (TDDFT)[23−26] and semiempirical Zerner intermediate neglect of differential overlap (ZINDO)[27,28] calculations were performed using Gaussian 09.[29] The hybrid B3LYP,[30] BH&HLYP,[31,32] and PBE0[33] functionals and the long-range corrected CAM-B3LYP[34] functional were used. The two Ahlrichs basis sets SVP and TZVP[35,36] were employed, in addition to a version of TZVP (aug-TZVP) augmented with a set of (1s1p1d/1s1p) functions taken from the most diffuse functions of aug-cc-pVDZ.[37] CD spectra were generated from computed rotational strengths using SpecDis software[38] with exponential half-width (half-width at 1/*e* height) σ = 0.3 eV, corresponding to Δ = 64 nm at 510 nm.

Exciton Calculations. Exciton calculations were run using the equations reported in the Supporting Information (eqs S6−S49), employing the spectroscopic and geometric parameters for the 570 nm transition summarized in Table 3. The direction of the electric dipole transition moment and the magnitude and direction of the magnetic dipole transition moment were derived from the TDDFT calculations. The electric dipole transition moment was centered at the origin of the retinal PSB coordinate system used in the TDDFT calculations, a point near C_8 and C_9 of the retPSB chromophore (Table S1, Supporting Information).

DeVoe Calculations. DeVoe polarizability theory[39,40] calculations were employed to estimate the intra- and intertrimer exciton couplings between the first 570 nm transition of retPSB chromophores. The calculations were run using eq S59 in the Supporting Information (specific for a trimer) and a computer routine due to W. Hug[41] (for all aggregates). The transition dipole was centered on C_9 and directed along the C_7−C_{15} direction. The band-shape (eq S50, Supporting Information) was either modeled on the visible absorption spectrum of bR[14] or approximated by a Gaussian band obtained by least-squares fitting of the experimental data (see Table 1). A unit dielectric constant was used in the calculations.

Table 1. Experimental Spectroscopic Data for Bacteriorhodopsin[a]

	α	β	γ
λ_{max}[b] (nm)	**568**,[8,14,44] **567**[95]	**318**,[5] **317**,[14] 320[45]	**263**,[5] 260[6,45]
ε_{max} (M^{-1} cm^{-1})	**63000**,[44] **56000**[8]		
Δ[c] (nm)	64,[9] **57**,[80] **60**[45]	27,[45] 28[6]	20[c]
$\lvert\mu\rvert$[d] (D)	**10.4**,[14] 10.7,[i] **10.2**,[8] **11**,[j] **9.8**[45]		
θ[e] (deg)	**71** or **78**,[67] 66.5,[68] 64.5[69]		
$\Delta\varepsilon_{max}$[f] (M^{-1} cm^{-1})	−13.3, +17.9;[6] −15.9, +31.3;[7] −9.0, +16.7;[14] −9.9, +16.1;[45] −8.4, +14.4[46]	−18.5,[6] −16.8[45]	22.8,[6] +12.2[45]
R[g] (DBM)	**0.32**,[14] **0.05**[8]	−0.71,[6] −0.62[45]	0.75,[6] 0.44[45]
S_{exp}[h] (M^{-1} cm^{-1})	**−24.9**,[2] −22.8,[46] −26.0,[45] −31.2,[6] −47.2,[7] −22.6,[1] −25.7[12]		

[a]Values in bold are explicitly stated in the references cited. Other values were read from published graphs or calculated from values reported or estimated from graphs. [b]For the visible band, λ_{max} is from the absorption spectrum. For the ultraviolet bands, it is from the CD spectrum. [c]Half of the bandwidth at 1/e of the maximum. For the visible bands, this is reported or estimated from the absorption spectrum. For the 320 nm band, it is estimated from the CD spectrum. For the 260 nm band, it is calculated from the empirical equation[96] $\Delta = k\lambda^{1.5}$, with k = 0.00470 evaluated from the value for the visible band. This method gives agreement with the observed value for the 320 nm band. [d]Magnitude of the electric dipole transition moment, calculated from ε_{max} and Δ assuming a Gaussian band shape. [e]Angle of the 570 nm transition dipole moment with respect to the 3-fold axis, determined from linear dichroism. This is often reported as its complement, the angle of the transition moment with respect to the plane of the membrane. [f]For the visible band, the first value is that for the long-wavelength band and the second value is for the short-wavelength band. [g]Rotational strength. 1 DBM = 0.9273 × 10^{-38} cgs units. The value for the visible band is the sum of the two bands of opposite sign. For the UV bands, R is calculated from $\Delta\varepsilon_{max}$ and Δ assuming a Gaussian band shape. [h]The couplet strength is defined as $\Delta\varepsilon_{\lambda+} - \Delta\varepsilon_{\lambda-}$, where $\Delta\varepsilon_{\lambda+}$ is $\Delta\varepsilon_{max}$ at the long-wavelength maximum and $\Delta\varepsilon_{\lambda-}$ is that at the short-wavelength maximum of a couplet. [i]Calculated from the maximum extinction coefficient of Oesterhelt and Hess[44] and the bandwidth of Kriebel and Albrecht.[9] [j]Calculated by Ebrey et al.[8] from the data of Oesterhelt and Hess.[44]

Extrinsic Coupling Calculations. The coupling between retPSB transitions and aromatic and peptide groups was evaluated by means of first-order perturbation theory[42] using eqs S62−S74 in the Supporting Information. All coupling contributions were evaluated in the monopole approximation (eq S40), using scaled Mulliken charges (see the Supporting Information) from CAM-B3LYP/SVP calculations for the 570 nm transition in the retinal and transition monopoles for the peptide and aromatic transitions from Woody and Sreerama.[43] Other transition parameters for the retinal are given in Tables 1

dx.doi.org/10.1021/jp212166k | J. Phys. Chem. B 2012, 116, 6751−6763

and 3. The calculations were performed for a trimer and, to approximate a two-dimensional crystal, for a 21-mer consisting of a central trimer and six neighboring trimers.

RESULTS

Experimental spectroscopic data for bacteriorhodopsin in light-adapted (with all-trans retPSB) purple membrane are summarized in Table 1 and shown in Figure 1. The primary

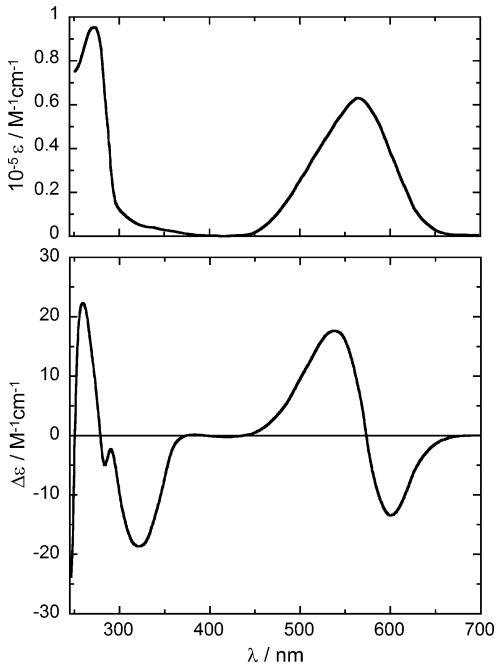

Figure 1. Experimental absorption UV−vis (top) and CD spectra (bottom) of bacteriorhodopsin. The absorption spectrum is taken from Wu and El Sayed[14] and normalized using the ε_{max} value of Oesterhelt and Hess.[44] The CD spectrum was taken from Heyn et al. and is normalized per monomer.[6]

spectroscopic data for the visible band (also indicated as the α-band) consist of the center of the absorption band, λ_0 = 570 nm,[44] its maximum intensity, ε_{max} = 63000 M^{-1} cm^{-1},[44] and the Gaussian bandwidth, Δ = 64 nm.[9] With these parameters, assuming a Gaussian band shape, the electric dipole transition moment is calculated to be 10.7 D. The couplet strength S of the visible band, namely, the peak-to-trough vertical amplitude of the couplet, can be calculated from many reports,[1,2,6,7,12,45,46] with a consensus value of S_{exp} = −25 M^{-1} cm^{-1} per monomer. The higher energy transitions of the retPSB have been studied less intensively, but data for the second and third electronic transitions are available.[6,45] These transitions give rise to a negative CD band near 320 nm and a positive one near 260 nm, indicated respectively as the β- and γ-bands (Figure 1).

DFT and ZINDO Calculations on Isolated retPSB. Retinal and its analogues, including truncated models and/or their Schiff bases (protonated, PSB, or not), have been extensively investigated by quantum mechanical calculations, especially with the aim of elucidating the spectral tuning and photodynamic processes of visual pigments.[47] Various DFT functionals have been demonstrated to well predict the first excitation energies and oscillator strengths of retinoids and their PSBs.[48−58] An increase of the Hartree−Fock exchange fraction as in the BH&HLYP functional[21,57] and, especially, the use of long-range corrected CAM-B3LYP[58−60] are also known to relieve the problems connected to the simulation of the S_1 geometry of PSB which affect standard functionals,[47,48,51,56,58] and remain effective in estimating excitation energies and moments. For comparison with present and previous literature results, ZINDO calculations were also performed on retPSB monomer and trimers.[21,53] For extensive discussion on the computational methods employed, with special attention to the choice of functional and basis set, see the Supporting Information.

Table 2 reports TDDFT-calculated data for the first transition of all-trans retPSB with various functionals and

Table 2. Computed $S_0 \rightarrow S_1$ Transition Parameters for retPSB Monomer[a]

method	basis set	λ_{max} (nm)	$E_{0\rightarrow1}$ (eV)	f	R_{DL}[b] (DBM)	R_{DV}[c] (DBM)
BH&HLYP	SVP	501.5	2.47	1.55	−0.231	−0.236
CAM-B3LYP	SVP	510.9	2.43	1.53	−0.232	−0.234
CAM-B3LYP	TZVP	519.3	2.39	1.53	−0.206	−0.214
CAM-B3LYP	aug-TZVP	502.8	2.38	1.53	−0.217	−0.215
PBE0	SVP	554.2	2.24	1.26	−0.177	−0.181
B3LYP	SVP	567.0	2.19	1.17	−0.160	−0.164
B3LYP	TZVP	574.5	2.16	1.19	−0.133	−0.142
ZINDO	VSTO-6G	573.3	2.16	1.61	−0.225	−0.201

[a]Input geometry obtained from the X-ray structure of purple membrane (PDB code 1C3W).[10] [b]Rotational strength calculated with the dipole-length (DL) gauge. [c]Rotational strength calculated with the dipole-velocity (DV) gauge.

basis sets, and ZINDO results for comparison, using a geometry generated from the X-ray crystal structure (PDB code 1C3W)[10] as described in the Methods section. Similar results for another X-ray structure (PDB code 1QM8)[19] are listed in the Supporting Information, Table S2. The effect of the basis set is only minor for all computed quantities, and the smallest basis set (SVP) almost leads to basis set completeness.[61] On the contrary, the choice of the functional has a moderate impact on both the transition energy $E_{0\rightarrow1}$ (2.16−2.47 eV) and the oscillator strength f (1.17−1.61). The calculated transition energy $E_{0\rightarrow1}$ is in the order BH&HLYP $\gtrsim$ CAM-B3LYP > PBE0 > B3LYP; that is, it follows the order of the Hartree−Fock exchange fraction HF-X, as anticipated.[53,57,58,62] In terms of matching of experimental transition energies and oscillator strength (Table 1), the hybrid functionals B3LYP and PBE0 with smaller HF-X perform better than BH&HLYP and CAM-B3LYP. Interestingly, ZINDO results are especially close to the experimental transition energy, but the oscillator strength is overestimated more than by any TDDFT method. It must be recalled that the present calculations were run on a protonated retPSB model and *in vacuo*. The presence of a single counterion or negative point charge may affect retPSB transitions significantly.[57] However, the protein matrix seems to counterbalance this local effect[63] in such a way that the overall impact of environmental effects, estimated, e.g., with the ONIOM-(QM:MM) model, leads to only a modest red-shift (10−15 nm) for the first computed transition of rhodopsin (Rh) and bR.[62,64] In consideration of the good performance of CAM-B3LYP in the overall description of the first excited state of retinoid PSB,[58−60] we chose the CAM-B3LYP/SVP method as a reference.

dx.doi.org/10.1021/jp212166k | J. Phys. Chem. B 2012, 116, 6751−6763

The first ($S_0 \rightarrow S_1$) transition, calculated at 510.9 nm (2.43 eV) by CAM-B3LYP/SVP, is mainly a HOMO → LUMO $\pi\pi^*$ excitation (Kohn−Sham orbitals are shown in Figure 2). In keeping with literature results,[21,52,54,56,57,65,66] population analysis revealed that an electron displacement occurs from the β-ionone side toward the iminium side of retPSB, or, in different terms, the positive charge moves toward the β-ionone side. Halving the molecule at the $C_{11}-C_{12}$ bond,[21,66] the fraction of positive charge on the right half (from C_{12} to the iminium) is 63% for the S_0 state and 30% for the S_1 state, respectively, in good accord with CASSCF results.[66] The calculated difference $\Delta\mu_{0\rightarrow1}$ between S_1 and S_0 dipole moments is directed toward the β-ionone and its absolute value is 18.2 D (using Mulliken charges), which also compares well with experimental data.[65] The direction of the transition moment is predicted to make an angle of 111° with respect to the 3-fold axis of bR trimers (Table 3), equivalent to 69°, in good agreement with experimental values (65−78°, Table 1).[67−69]

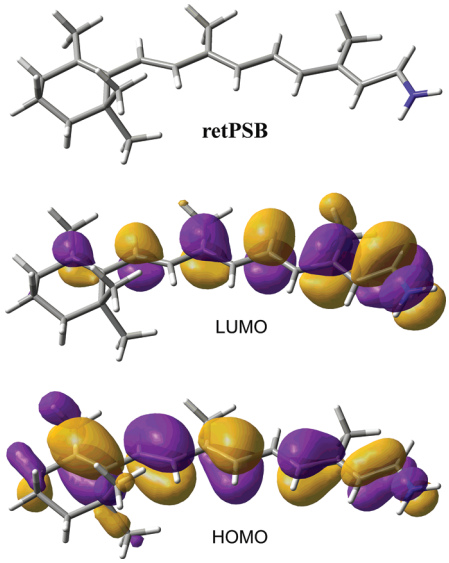

Figure 2. Computed Kohn−Sham orbitals at the CAM-B3LYP/SVP level for retPSB.

With all methods considered, the second calculated transition $S_0 \rightarrow S_2$ for retPSB is 1−1.4 eV higher in energy (blue-shifted by 130−180 nm) than the $S_0 \rightarrow S_1$ one; it is due to a HOMO-1 → LUMO $\pi\pi^*$ excitation and is associated with a moderate oscillator strength, f = 0.2−0.5 (see Table S4, Supporting Information). This result is in agreement with previous theoretical outcomes.[49,51,55,60,66,70] The large energy separation between the first two calculated transitions is at odds with the proposal that the bisignate CD of bR in the α-band region is due to two distinct low-lying transitions.[1,12,15,16]

The calculated rotational strength for the α band of retPSB, corresponding to the intrinsic chirality of the chromophore, is negative and small for all methods considered (between −0.13 and −0.23 DBM, 1 DBM = 0.9273×10^{-38} cgs units) (Table 2 and Figure 3). It is similarly negative and smaller for 1QM8 geometry (between −0.06 and −0.08 DBM) (Table S2, Supporting Information). The small value for the intrinsic rotational strength is not surprising, because the chromophoric system is almost planar in the bR retPBS chromophore. In fact, the root-mean-square deviation from the average plane for the

Table 3. Spectroscopic and Structural Parameters for the Bacteriorhodopsin α Band[a]

μ^b (D)	10.7
$\lambda_0{}^b$ (nm)	570
Δ^b (nm)	64
r^c (Å)	17.78
θ^d (deg)	110.99
ϕ^e (deg)	166.79
Im m^f (BM)	0.9154
$\theta_m{}^g$ (deg)	71.71
$\phi_m{}^h$ (deg)	250.78
V^i (cm^{-1})	−11.73
ΔE^j (cm^{-1})	−35.20
$\delta\lambda^k$ (nm)	1.14
$R_+{}^l$ (DBM)	−33.99
S^m (M^{-1} cm^{-1})	−21

[a]Calculated data are extracted from TDDFT calculations at the CAM-B3LYP/SVP level. For corresponding results on high-energy transitions and ZINDO-derived results, see Table S5 in the Supporting Information. [b]From ε_{max} = 63000 M^{-1} cm^{-1} (ref 44) and λ_0 = 570 nm (ref 44 gives 568 nm), bandwidth Δ = 64 nm, assuming a Gaussian band shape. Reference 8 gives μ = 10.2 D, based upon a smaller ε_{max} = 56000 M^{-1} cm^{-1} and bandwidth of 63 nm. [c]r is the distance of the center of the retinal PSB chromophore from the 3-fold axis of the trimer. From the crystal structure (PDB code 1C3W).[10] [d]The angle between the electric dipole transition moment and the 3-fold z-axis, from TDDFT calculations. [e]The angle between the projection of the electric dipole transition moment in the xy-plane and the $+x$-axis, from TDDFT calculations. [f]The magnitude of the magnetic dipole transition moment in Bohr magnetons. The magnitude and direction of **m** are obtained from TDDFT calculations. [g]The angle between the magnetic dipole transition moment and the 3-fold z-axis, from TDDFT calculations. [h]The angle between the projection of the magnetic dipole transition moment in the xy-plane and the $+x$-axis, from TDDFT calculations. [i]Total exciton coupling energy between nonequivalent transition moments in the crystal (see eq S47 in the Supporting Information). [j]Exciton splitting energy in crystal. Energy of A component minus that of E component. See eq S49 in the Supporting Information. [k]Exciton splitting on the wavelength scale. [l]Mean exciton rotational strength with the sign of the long-wavelength component. [m]Couplet strength, eq 1.

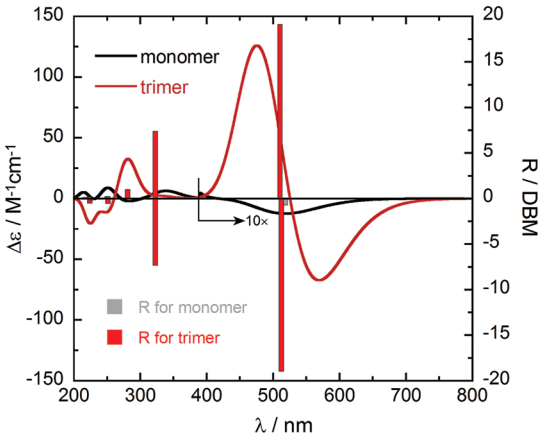

Figure 3. Calculated CD spectrum with CAM-B3LYP/SVP on the retPSB monomer and trimer. Vertical bars represent computed rotational strengths in DBM. The spectrum and bars for the monomer are magnified above 390 nm. To compare intensity values with those in the tables and in Figures 4 and 7, the intensity must be divided by 3.

dx.doi.org/10.1021/jp212166k | J. Phys. Chem. B 2012, 116, 6751−6763

Table 4. Computed 570 nm Couplet Parameters for retPSB Trimer[a]

method	basis set	λ_{max} (nm)	E (eV)	$3V_{ab}$ (eV) [$\delta\lambda$ (nm)]	f	R_{DL}[b] (DBM)	R_{DV}[b] (DBM)	S[c] (M^{-1} cm^{-1})
CAM-B3LYP	SVP	512.25	2.420	−0.010 [2.1]	0.59	−62.3	−61.1	−63.6
		510.19	2.430		4.00	63.3	60.6	
PBE0	SVP	555.52	2.232	−0.008 [2.0]	0.59	−56.2	−54.7	−58.8
		553.50	2.240		3.18	56.5	54.3	
B3LYP	SVP	568.21	2.182	−0.008 [2.1]	0.56	−53.3	−52.2	−60.0
		566.23	2.190		2.96	53.6	51.5	
ZINDO	VSTO-6G	575.80	2.153	−0.013 [3.5]	0.44	−41.8	−37.2	−80.8
		572.41	2.166		4.40	52.4	36.6	

[a]Input geometry obtained from the X-ray structure of purple membrane.[10] [b]Normalized per monomer. [c]Couplet strength, from eq 1, using for R_+ the average of the four values (R_{DL} and R_{DV} for two transitions), and the exponential half-width σ corresponding to Δ = 64 nm at the computed λ_{max} (for the first line, σ = 0.3 eV).

polyeneimine systems (from C_6 to N) is 0.174 Å for the 1C3W structure and 0.060 Å for the 1QM8 structure, respectively.

DFT and ZINDO Calculations on retPSB Trimers. Data from TDDFT (with CAM-B3LYP, B3LYP, and PBE0 functionals and SVP basis set) and ZINDO calculations on trimers of retPSB as found in the crystals of bR are reported in Tables 4 (1C3W structure) and S3 (Supporting Information) (1QM8 structure). To the best of our knowledge, these are the first excited-state quantum-mechanical calculations on retPSB trimers. The results are quite robust to the method employed. In all cases, in fact, three close-lying transitions are predicted as the first excitations with non-negligible dipolar and rotational strengths. With CAM-B3LYP and ZINDO, these also represent the first three excitations; with B3LYP and PBE0, they are preceded by a few spurious excitations with zero dipolar and rotational strengths. The first excitation has A symmetry, while the second and third excitations are two degenerate excitations with E symmetry and can be considered altogether as a single (second) transition. The energy difference between the two transitions is 8−10 meV (64−80 cm^{-1}), and the ratio between oscillator strengths is 5.3−6.8 with TDDFT, the second transition being always the most intense one with a total f between 1.0 and 1.5 per monomer. Very importantly, the two transitions are allied with strong rotational strengths, opposite in sign and similar in magnitude, between −37 and −63 DBM for the first transition and +37 to +63 DBM for the second (combination of two). In practice, the calculated CD spectrum with all methods corresponds to a strong negative exciton couplet in the long-wavelength region. With all functionals employed, the two rotational strengths are very close in intensity (see Table 4) and a symmetrical CD couplet is obtained (see Figure 3 for the CAM-B3LYP/SVP result). Population analysis further confirms the exciton nature of the three excited states and reflects the three-state picture implied by the exciton model (see the Supporting Information). In particular, the symmetry, degeneracy, and wave function description of the three states faithfully follow eqs S6−S8 in the Supporting Information. Electric and magnetic transition moments for the first, A-symmetry, excitation are parallel to each other, both directed along the C_3 symmetry axis. On the contrary, electric and magnetic transition moments for the following degenerate pair of transitions, with E symmetry, are both polarized in the plane perpendicular to the C_3 axis.

The exciton couplet strength predicted by quantum-mechanical calculations on the trimer ($S_{3,QM}$) can be evaluated from the following equation:[4]

$$S = \Delta\varepsilon_{\lambda+} - \Delta\varepsilon_{\lambda-} = 3.92R_+\delta\lambda\,\lambda_0/\Delta^2 \quad (1)$$

using TDDFT or ZINDO calculated values for three parameters, R_+ (rotational strength of the long-wavelength exciton component in DBM), $\delta\lambda$ (exciton splitting in nm), and λ_0 (center of gravity of the exciton bands in nm, taken to be the absorption maximum), and the experimental value Δ = 64 nm; the resulting values are listed in Table 4. The three TDDFT methods consistently predict $S_{3,QM}$ between −59 and −64 M^{-1} cm^{-1} (here and in the following, couplet strengths are normalized per monomer). This value is about 2 times larger than that calculated by the exciton approach (see below). The two values can be reconciled recalling the overestimation of the calculated transition dipole moment for monomeric retPSB (12.9 D with CAM-B3LYP/SVP) with respect to the experimental value (10.7 D) used in the exciton calculations. Since the couplet intensity is proportional to the squared dipole strength (fourth power of transition dipole moment),[71] a ratio of $(12.9/10.7)^4$ = 2.1 is expected between the $S_{3,QM}$ and $S_{3,exc}$ values.

Exciton Calculations. Exciton calculations were run using the equations reported in the Supporting Information on both an "isolated" retPSB trimer (eqs S6−S43) and an infinite crystal of retPSB chromophores, as found in the purple membrane (eqs S44−S49). The exciton coupling energy V_{ab} was calculated either with the point-dipole approximation (eq S39) or the monopole approximation (eq S40).

The point-dipole approximation using the empirical transition moment magnitude of 10.7 D (Table 1) and the TDDFT transition moment direction (Table 3) gives the exciton coupling energy V_{ab} = −16.27 cm^{-1} and an exciton splitting of E_{exc} = $3V_{ab}$ = −48.81 cm^{-1}, corresponding to a splitting $\delta\lambda$ = 1.59 nm for the trimer. It should be noted that the negative sign for the dipole−dipole coupling contradicts the assignment made by Ebrey et al.,[8] who concluded that the coupling energy must be positive. A negative value for V_{ab} implies that the A state is at lower energy than the E state, in accord with the quantum-mechanical calculations discussed above. Using the more accurate monopole approximation (eq S40, Supporting Information) and the scaled Mulliken charges, we obtain V_{ab} = −17.70 cm^{-1}, corresponding to $\delta\lambda$ = 1.73 nm for the exciton splitting in the trimer. For the bR crystal (the purple membrane), we must take into account intertrimer interactions using eq S49 (Supporting Information). In the monopole approximation, we obtain

$$\sum_n V_{11,2n} = -11.73\ cm^{-1} \quad (2)$$

where $V_{11,2n}$ is the Coulomb interaction potential between the transition moment in monomer 1 of trimer 1 and that of

dx.doi.org/10.1021/jp212166k | J. Phys. Chem. B 2012, 116, 6751−6763

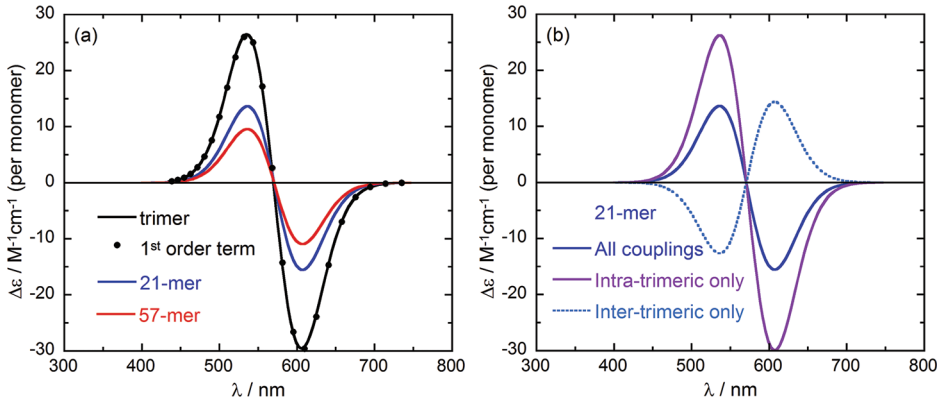

Figure 4. Calculated CD spectrum with DeVoe's method on three different aggregates of retPSB with geometries deduced from the X-ray structure of bR.[10] (a) Comparison between a trimer, a 21-mer (7 trimers), and a 57-mer (19 trimers); see structure in Figure 5. Circles represent the spectrum calculated at first order for the trimer rather than at all orders. (b) Comparison between various coupling terms for the 21-mer. All spectra are normalized per monomer.

monomer 2 in trimer *n*. Thus, the exciton splitting in the crystal is $\Delta E_{exc} = -35.20$ cm^{-1}, giving $\delta\lambda = 1.14$ nm. Note that the splitting for the crystal is about 2/3 that for the trimer. This results from intertrimer couplings that are opposite in sign to the intratrimer couplings. The DeVoe theory calculations (see below) give a similar picture in which the interactions between trimers diminish the amplitude of the overall CD couplet relative to that within a trimer.

The rotational strengths for the two exciton components were calculated from eqs S33−S36 (Supporting Information). The $\mu-\mu$ contribution to the exciton rotational strengths are, per monomer,

$$R_{\mu\mu A} = -39.40 \text{ DBM} \quad (3)$$

$$R_{\mu\mu E1} = R_{\mu\mu E2} = +19.70 \text{ DBM} \quad (4)$$

The $\mu-$m contributions to the exciton rotational strengths were calculated from eqs S35 and S36 (Supporting Information):

$$R_{\mu mA} = -1.1011 \text{ DBM} \quad (5)$$

$$R_{\mu mE1} = R_{\mu mE2} = +0.4545 \text{ DBM} \quad (6)$$

Note that the $\mu-$m contributions do not sum to zero as the $\mu-\mu$ contributions do. Their sum is −0.1921 DBM, which is the intrinsic rotational strength of the retinal retPSB chromophore. (This differs from the value given in Table 2 for CAM-B3LYP/SVP results because the electric dipole transition moment has been scaled down to the empirical value of 10.7 D from the TDDFT value of 12.90 D.) The two exciton bands therefore have rotational strengths of

$$R_A = -39.40 - 1.10 = -40.50 \text{ DBM} \quad (7)$$

$$R_E = R_{E1} + R_{E2} = 2(19.70 + 0.45) = +40.30 \text{ DBM} \quad (8)$$

The mean rotational strength magnitude is 40.40 DBM, and this yields a predicted couplet strength of $S_{3,exc} = -38$ M^{-1} cm^{-1} for the trimer and $S_{\infty,exc} = -25$ M^{-1} cm^{-1} for the crystal. As noted above, these values are consistent with TDDFT data if the different dipole strength values are taken into account.

DeVoe Calculations. DeVoe's polarizability theory[39,40] provides a method based on classical physics for the calculation of absorption and CD spectra of an aggregate of damped oscillators, which represent transition dipoles in quantum-mechanical terms. DeVoe's method has been successfully applied in several cases of multichromophoric compounds, including organic compounds,[72] biopolymers and prosthetic groups,[73] and macromolecules and supramolecular architectures.[74−76] The major advantages of DeVoe's method are that it is an all-order method and it explicitly takes into account band shapes. This is especially useful in the so-called weak-coupling case,[77] that is, when the coupling interaction potential V_{ab} is much smaller than the inherent bandwidth, for example, because of large distances as in the case of bR. In the standard strong-coupling exciton treatment, in fact, the spectral band shape and/or bandwidth of the chromophore absorption is neglected; energy levels, transition dipoles, and rotational strengths are estimated for the aggregate, and only thereafter is a band shape applied.[78] With the DeVoe method, instead, the true absorption spectrum of the chromophore or a suitable band-shape function (in the current case, a Gaussian curve) may be used.[41]

The results of DeVoe calculations (see the Supporting Information, eqs S50−S55) for 1, 7, and 19 bR trimers are shown in Figure 4a. They correspond to a 3-mer, a 21-mer, and a 57-mer aggregate of retPSB units, respectively, as depicted in Figure 5. The CD spectrum for the trimer, calculated with DeVoe theory at all orders, consists of a negative couplet with extrema at 535 and 607 nm and couplet strength $S_{3,DeV} = -56$ M^{-1} cm^{-1} per monomer. This should be compared with the value of −38 M^{-1} cm^{-1} from the exciton model for a single trimer. Inclusion of further trimers in the calculations leads again to a negative couplet with the same shape as that for a single trimer, although with reduced intensity. For seven trimers, the couplet strength per monomer is $S_{21,DeV} = -29$ M^{-1} cm^{-1}, and for 19 trimers, $S_{57,DeV} = -21$ M^{-1} cm^{-1}. The latter value agrees well with the experimental value for the purple membrane ($S_{exp} = -25$ M^{-1} cm^{-1}). Each value agrees satisfactorily with the corresponding result from exciton theory: $S_{21,exc} = -32$ M^{-1} cm^{-1} for the 21-mer and $S_{\infty,exc} = -25$ M^{-1} cm^{-1} for the infinite crystal. Explicit evaluation of intratrimeric and intertrimeric couplings was run for the 21-mer (Figure 4b). The effect of intratrimeric terms (21 distinct pairwise couplings) is obviously coincident with the negative couplet obtained for the 3-mer. The intertrimeric terms (189 pairwise couplings) give rise to a positive couplet with almost half the amplitude of the intratrimeric one. Thus, the average intertrimeric coupling is much weaker than the intratrimeric

dx.doi.org/10.1021/jp212166k | J. Phys. Chem. B 2012, 116, 6751−6763

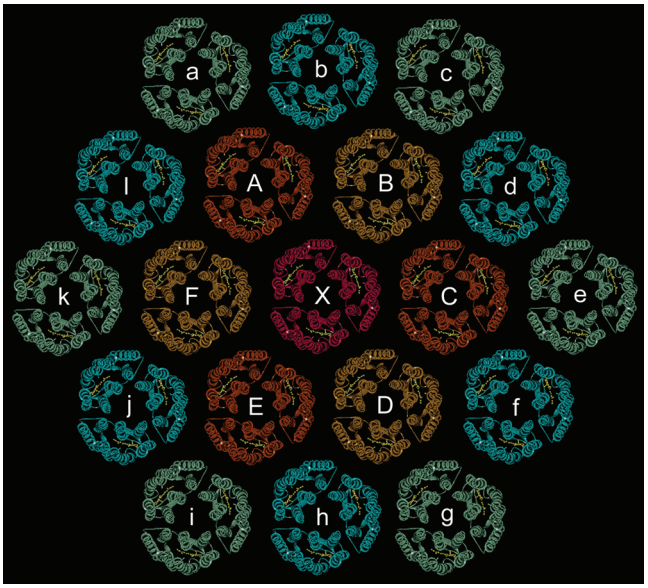

Figure 5. Arrangement of bR trimers in the X-ray crystal structure of the purple membrane seen along the normal to the membrane. retPSB chromophores are depicted in yellow. The central trimer (X) is surrounded by a "first sphere" ensemble of 6 trimers (A–F), constituting a 21-mer (7 trimers), and a "second-sphere" ensemble of 12 trimers (a–l), constituting a 57-mer (19 trimers).

one, but the combined effect of many intertrimeric terms reduces the amplitude of the overall couplet by a factor of ~2. This result is consistent with that obtained with exciton calculations.

If the experimental band shape is used in DeVoe calculations instead of a Gaussian band shape (Figure S2, Supporting Information), a negative couplet is again obtained. Because of the asymmetry of the experimental band shape, the resultant couplet is not symmetrical and the negative branch is more pronounced than the positive one. The calculated couplet strengths for the various aggregates are $S_{3,DeV} = -55\ M^{-1}\ cm^{-1}$, $S_{21,DeV} = -28\ M^{-1}\ cm^{-1}$, and $S_{57,DeV} = -20\ M^{-1}\ cm^{-1}$ for the trimer, the 21-mer, and the 57-mer, respectively, only a little smaller than those obtained with the Gaussian band shape.

The CD spectrum of the trimer was also calculated using explicit eqs S58 and S59 derived from a perturbative treatment, truncated at the second order, of DeVoe's approach (see the Supporting Information). This simplification led to exactly the same CD as the all-order calculation (Figure S3, Supporting Information). Even the truncation at the first order led to a calculated CD superimposable to the all-order one (Figure 4a). This is because the small coupling interaction makes the second-order term of eq S59 (Supporting Information) almost negligible. It is noteworthy that a very simple equation such as eq S59 (Supporting Information) truncated at the first term may be used to calculate the exciton-coupled spectrum of a multichromophoric aggregate belonging to a weak-coupling case, taking fully into account the natural band shape.

Calculations of Extrinsic Coupling. In the analysis of Ebrey et al.[8] and in other discussions of the 570 nm band of bR, it has been assumed that the intrinsic CD of the chromophore and the contributions from coupling with aromatic and peptide groups give rise to a single band at the unperturbed wavelength of the chromophore, in contrast to the couplet that arises from the exciton effect. In fact, each of the exciton components will couple with other protein chromophores and will have contributions from the intrinsic chirality. The rotational strengths from these sources may be of opposite sign for the two exciton components, giving rise to a couplet that will either reinforce or partially cancel the exciton couplet. Interestingly enough, the quantitative impact of this extrinsic coupling has never been evaluated before for bR.

The contributions of coupling between the exciton levels of the 570 nm band and the aromatic and peptide groups were calculated using eqs S62–S64 (Supporting Information). The calculations were performed for the trimer and a 21-mer (7 trimers, see Figure 5), which is expected to well approximate the infinite crystal. Further details of the coupling contributions of the aromatic side chains and the peptide groups are presented in Tables S6 and S7, respectively, in the Supporting Information.

As seen in Table 5, the aromatic side chains make a significant contribution to the exciton rotational strengths of

Table 5. Intrinsic and Coupling Contributions to Exciton Rotational Strengths for the 570 nm (α-) Band[a]

	A	E[b]	net[c]
	Trimer		
intrinsic $\mu-\mu$	−39.3950	19.6975	0
intrinsic μ–m	−1.1011	0.4545	−0.1921
aromatic	6.3002	−2.9131	0.4741
peptide	−0.4304	0.1332	−0.1639
$\beta + \gamma$[d]	−0.0054	0.0021	−0.0013
total	−34.6317	17.3742	0.1168
	21-mer		
intrinsic $\mu-\mu$	−39.3950	19.6975	0
intrinsic μ–m	−1.1011	0.4545	−0.1921
aromatic	6.7184	−3.1155	0.4874
peptide	−0.0905	0.0154	−0.0597
$\beta + \gamma$[d]	−0.0054	0.0021	−0.0013
total	−33.8736	17.0540	0.2343

[a] $\mu-\mu$ refers to coupling of the electric dipole transition moments among the retinal chromophores of the trimer (eqs S33 and S34, Supporting Information). μ–m refers to the coupling of the electric moment of a retinal with both its own magnetic moment and the magnetic moments of the other two retinals in the trimer (eqs S35 and S36, Supporting Information). All results are given per retinal. [b] The E exciton components are degenerate and have equal contributions from all sources. [c] The net contribution is the sum of the A value plus twice the E value. [d] Sum of the contributions from coupling of the α-band with the β- and γ-bands.

the trimer: +6.30 DBM to the A component and −2.91 DBM to each of the E components, with a net contribution of +0.47 DBM. The coupling with the aromatic side chains is in the opposite sense to the intrinsic exciton intensity and therefore diminishes the exciton band amplitude. The resultant is a small fraction (~7%) of the magnitude of the coupling contributions to either exciton component. This demonstrates that the assumption that nonexciton rotational strength contributions give rise to a single Gaussian band is not correct.

Table 5 also shows the effects of coupling with the peptide chromophores in the trimer. These are smaller by an order of magnitude than those from the aromatic side chains: −0.43 DBM to the A component and +0.13 DBM to each of the E components, giving a net contribution of −0.16 DBM. The peptide $\pi\pi^*$ transitions are responsible for most of this effect.

Table 5 also shows the aromatic and peptide contributions to the exciton rotational strengths of the 21-mer. These are similar

dx.doi.org/10.1021/jp212166k | J. Phys. Chem. B 2012, 116, 6751–6763

to those for the trimer, as the coupling between retPSB chromophores in one trimer and the aromatic chromophores in a different trimer is substantially weaker than the intratrimer coupling. Table S6 (Supporting Information) compares the contributions of intra- and intertrimer couplings with aromatic side chains in the 21-mer. The intertrimer coupling contribution is weaker by an order of magnitude than the intratrimer coupling, despite the fact that the number of contributing groups is 6-fold greater in the former case. For peptide groups (Table S7, Supporting Information), there is a much smaller difference between the intra- and intertrimer couplings in the case of the dominant $\mu-\mu$ coupling.

Nearby aromatic groups make the largest contributions to the rotational strength. Table 6 lists the side chains within a trimer that contribute more than ±0.05 DBM to the net rotational strength of the 570 nm transition. All but three are within the same monomer, but it will be noted that even side chains with centers up to 30 Å from the center of the retPSB center may not be negligible. Figure 6 shows the retPSB chromophore and the aromatic side chains listed in Table 6 that make contributions larger than ±0.05 DBM.

Table 6. Principal Aromatic Side-Chain Contributions to the Rotational Strength of retPSB in Monomer A[a]

side chain	monomer[b]	distance[c] (Å)	contribution (DBM)
Tyr 79	A	15.4	0.0884
Trp 80	A	15.6	0.2159
Tyr 83	A	7.6	−0.0627
Trp 86	A	4.6	0.0816
Phe 88	A	14.2	0.0739
Phe 135	A	15.4	0.0591
Trp 138	A	10.1	−0.2432
Tyr 147	A	15.7	−0.1262
Tyr 150	A	19.2	−0.0840
Phe 153	A	16.6	0.0510
Trp 182	A	6.6	0.4368
Tyr 185	A	4.6	0.1881
Phe 219	A	13.8	0.1488
Trp 10	B	32.0	−0.0505
Trp 86	B	27.1	−0.0980
Tyr 137	C	22.5	0.0800

[a]Only aromatic groups that contribute more than 0.05 DBM in absolute value are included. [b]The retPSB chromophore is in chain A of the trimer, and the aromatic groups are in chains A, B, or C. [c]Center-to-center distance.

Combining the intrinsic and coupling contributions with the rotational strengths of the exciton levels in the trimer, we obtain (Table 5) rotational strengths of −34.63 DBM for component A and +17.37 DBM for each of the E components, with a net rotational strength of +0.12 DBM. The average magnitude of the exciton bands is predicted to be −34.69 DBM for the trimer and −33.99 DBM for the 21-mer approximating the infinite crystal. We can now predict the couplet strength for the trimer (eq 1):

$$S_{3,\mathrm{all}} = 3.92(-34.69)(1.725)(570)/64^2 = -33\ \mathrm{M}^{-1}\,\mathrm{cm}^{-1} \quad (9)$$

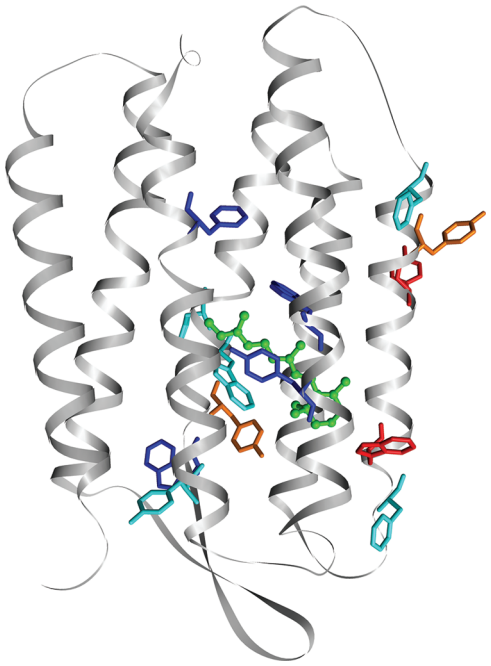

Figure 6. Aromatic side chains making the largest contributions to retPSB rotational strength. Only side chains from the same subunit are represented. The retPSB chromophore is green. Side chains are color coded according to their contributions: > +0.1 DBM, dark blue; +0.05 to +0.1 DBM, cyan; −0.05 to −0.1 DBM, orange; < −0.1 DBM, red.

For the crystal, the couplet strength is predicted to be

$$S_{\infty,\mathrm{all}} = 3.92(-33.99)(1.14)(570)/64^2 = -21\ \mathrm{M}^{-1}\,\mathrm{cm}^{-1} \quad (10)$$

This value is in good agreement with the consensus of experimental values, $S_{\mathrm{exp}} = -25\ \mathrm{M}^{-1}\,\mathrm{cm}^{-1}$ (Table 1). Figure 7 shows the predicted CD spectrum of the crystal in the visible region, as well as the two component bands. The individual components are very strong, but because of the small splitting, they largely cancel. The prediction of a more intense couplet for the isolated trimer than for the crystal is intriguing and could be tested if conditions for stabilizing such trimers can be

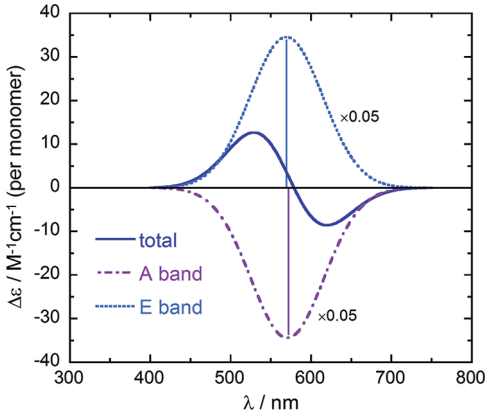

Figure 7. Predicted exciton spectrum of bacteriorhodopsin crystal. The total spectrum is shown in the solid line; the spectrum of the A band (divided by 20) is a dot-dashed line; that of the E band (divided by 20) is a dotted line. The rotational strengths are from Table 5 and include the exciton and coupling contributions.

dx.doi.org/10.1021/jp212166k | J. Phys. Chem. B 2012, 116, 6751−6763

found. The net rotational strength for the crystal is predicted to be +0.24 DBM, which falls between the two reported values of +0.05 and +0.32 DBM (Table 1). It should be noted that consideration of coupling with protein groups, especially aromatic side chains, is essential to account for the observed net positive rotational strength of the 570 nm band because the intrinsic rotational strength of the band from TDDFT and ZINDO calculations is negative.

It is interesting to compare the relative magnitudes for the intrinsic rotational strength and the net coupling in bacteriorhodopsin with the corresponding values for rhodopsin.[21] In bR, the intrinsic rotational strength, −0.23 DBM (CAM-B3LYP/SVP), is opposite in sign and smaller in magnitude than the net rotational strength from coupling (+0.43 DBM for the crystal, +0.32 DBM for the trimer), whereas, in rhodopsin, the intrinsic rotational strength is predicted[21] to be +0.62 and the coupling contributions are −0.32 DBM. Thus, the coupling contributions for the two systems are comparable in magnitude but opposite in sign, whereas the intrinsic contributions are substantially larger in magnitude for rhodopsin than in bR, and also opposite in sign. The larger magnitude for the intrinsic rotational strength in rhodopsin can be attributed to the larger deviations from planarity in the *cis* PSB chromophore vs the *trans* PSB chromophore of bR (Chart 1). For the X-ray structure of rhodopsin with the best resolution (PDB code 1U19)[79] used in previous intrinsic rotational strength calculations,[21] the root-mean-square deviation from the average plane for the polyeneimine systems (from C_6 to N) is 0.94 Å (for both PSB units), to be compared with 0.174 Å for the 1C3W structure of bR.

Higher Energy Transitions. The assignment and interpretation of the high-energy CD bands of bacteriorhodopsin (β, 320 nm, and γ, 280 nm, see Figure 1 and Table 1) is less straightforward than for the visible α band. Table S4 (Supporting Information) reports the data calculated with TDDFT and ZINDO for the $S_0 \rightarrow S_2$ and $S_0 \rightarrow S_3$ transitions, and Table S5 reports the relevant spectroscopic parameters. Contrary to the $S_0 \rightarrow S_1$ transition, the comparison with experimental data is ambiguous. In particular, the strong negative CD band observed at 320 nm[6,45] and the very small absorption band at 330−340 nm ($f < 0.01$) do not correlate with the predicted $S_0 \rightarrow S_2$ calculated transition. If the absorption and CD features in the 320−340 nm region are due to a retPSB-centered transition, they are not predicted by any of the calculation methods employed here. Because of the present uncertainty in the nature of the high-energy spectrum of bR, we prefer not to speculate on the calculation results and postpone the problem to future studies. Here, calculated data for $S_0 \rightarrow S_2$ and $S_0 \rightarrow S_3$ transitions were only employed to evaluate the necessary terms for their couplings with the $S_0 \rightarrow S_1$ transition (see eqs S65−S74 in the Supporting Information). As can be seen in Table 5, the overall contribution of these couplings to the calculated α band is negligible. In other words, the exciton coupling between retPSB chromophores in bR trimers and larger aggregates in the α-band region is almost entirely due to the degenerate coupling between $S_0 \rightarrow S_1$ transitions. This is because the exciton coupling between two nondegenerate transitions is directly proportional to the product of their dipolar strengths and inversely proportional to their energy difference and the cube of the distance.[71]

DISCUSSION

In the present study, we applied TDDFT calculations to predict the intrinsic rotational strength of the retPSB chromophore, and a combination of TDDFT parameters, coupled-oscillator theory, and DeVoe theory to predict the visible CD spectrum of bacteriorhodopsin. A strong negative couplet is consistently predicted by all methods to be associated with the 570 nm transition, with a couplet strength of $-21\ M^{-1}\ cm^{-1}$, in good agreement with the consensus from experiment. These results provide strong support for the original interpretation[1,5,6,8,80] that the visible CD spectrum of bacteriorhodopsin is generated by exciton coupling among the retPSB chromophores.

The experimental evidence for the exciton model has been clearly summarized by Heyn et al.[6] and by Cassim[15] and will not be repeated here. However, one line of evidence that we find especially impressive is the observation[7] that the negative couplet collapses to a single positive CD band when the CD is measured on films, with light propagating perpendicular to the plane of the membrane. This observation has a very simple explanation within the exciton model. For light propagating along the 3-fold (z) axis, the rotational strength arising from exciton coupling between the chromophores is proportional to the difference in the z-coordinates, $z_j - z_i$.[81] This factor vanishes for all of the exciton-coupled chromophores in the membrane. The collapse of the couplet for this direction of propagation is not readily explained within the alternative interpretations[11,12,14] of conformational heterogeneity or multiple transitions.

El-Sayed and co-workers published a series of papers strongly questioning the exciton interpretation.[11−14] Cassim[15] has provided a point-by-point response to the arguments of El-Sayed and co-workers against the exciton model. We are in general agreement with Cassim, but he emphasized a distinction between intratrimer and intertrimer exciton coupling that we do not consider to be essential. The principal arguments of El-Sayed[11,12,14] and other critics[16−18] of the exciton model will now be considered.

(1) An exciton splitting of ∼600 cm^{-1} and an interchromophoric distance of ∼12 Å were estimated by Ebrey et al.[8] However, the observed distance is at least 2-fold larger. Wu and El-Sayed[14] quoted 26 Å,[69] but the center-to-center distance from the X-ray structure by Luecke et al.[10] is ∼31 Å. Such distances lead to exciton splittings 10-fold smaller, too small in Wu and El-Sayed's view to give the observed couplet. However, two overlapping Gaussian bands of opposite sign and equal magnitude give a couplet with a peak-to-peak splitting that is determined solely by the bandwidth ($|\lambda_+ - \lambda_-| = \sqrt{2}\Delta$) and is independent of the separation of the Gaussian bands, $\delta\lambda$, when $\delta\lambda/\Delta \ll 1$.[80,82] Thus, exciton splittings as small as ∼1 nm will give rise to a couplet, the amplitude of which is determined by $R_+(\delta\lambda)$, the product of the rotational strength and the exciton splitting. If the exciton rotational strengths are sufficiently large, a couplet can readily be observed even for exciton splittings of the order of 1 nm.

Hasselbacher et al.[45] recognized this and analyzed their data for the 570 nm band by fitting the CD spectrum to two Gaussians. They obtained an exciton splitting of 33 cm^{-1} ($\delta\lambda$ = 1.1 nm) and a mean rotational strength magnitude of 78 DBM. The couplet strength (eq 1) calculated from these parameters, however, is $-53\ M^{-1}\ cm^{-1}$, twice their reported experimental value. The source of this discrepancy is not clear, but their work demonstrated that the 570 nm couplet is fully compatible with

dx.doi.org/10.1021/jp212166k | J. Phys. Chem. B 2012, 116, 6751−6763

a small exciton splitting and a large interchromophore distance. Our TDDFT-calculated CD spectra for the trimers also show intense exciton couplets with exciton splittings below 2 nm using Gaussian shapes with band widths of 0.25−0.3 eV (corresponding to Δ = 64 nm at the computed excitation wavelengths).

(2) Wu and El-Sayed[14] calculated the time t_{ET} required for energy transfer between chromophores from $t_{ET} = h/V$, where h is Planck's constant and V is the energy of interaction between the transition dipole moments, V_{ab} in eq S38 (Supporting Information), or $^1/_3$ of the exciton splitting. Taking V_{ab} = 200 cm^{-1},[8] Wu and El-Sayed reported $t_{ET} \sim$ 25 fs, a transfer time that is much shorter than the formation time for the first intermediate in the bR photocycle, ∼400 fs.[83,84] If energy transfer were this efficient, the first intermediate should show no linear dichroism. However, linear dichroism experiments demonstrate strong polarization of the K intermediate.[11,85] Using Wu and El-Sayed's equation, we calculate t = 167 fs, 7 times larger than the value reported by Wu and El-Sayed. Even this longer transfer time would lead to extensive depolarization before photochemistry.

We shall follow Kasha's[86] analysis of excitation transfer, according to which the time for excitation transfer is related to the exciton splitting:

$$t_{ET} = h/2\Delta E_{exc} \tag{11}$$

Our exciton calculations give $|\Delta E_{exc}|$ = 35.2 cm^{-1} for the purple membrane, so the time for excitation transfer using Kasha's formulation becomes t_{ET} = 480 fs, which is comparable to the formation time of the first photointermediate.[83,84] This time scale for energy transfer would still lead to significant but far from complete depolarization.

However, another factor needs to be considered. The excitation transfer time calculated above assumes *strong* exciton coupling in the sense of Simpson and Peterson,[77] i.e., $(\Delta E_{exc})/\Theta \gg 1$, where Θ is the vibronic bandwidth in cm^{-1}. With $|\Delta E_{exc}|$ = 35.2 cm^{-1} (this work) and Θ = 3250 cm^{-1},[9] we are clearly dealing with the opposite extreme, *weak* coupling. For weak coupling, the excitation transfer time is increased from $h/2\Delta E_{exc}$ by a factor of $[\sum_v \sum_{v'} g_v g_{v'} S_{vv'}{}^2]^{-1}$,[86] where v and v' are the vibrational levels in the excited and ground states, respectively; g_v and $g_{v'}$ are the fractional populations of the vibrational levels in the respective electronic states; and $S_{vv'}$ is the Franck−Condon factor, the overlap integral of the vibrational wave functions v and v'. In the present case, we can take vibrational relaxation to be complete before photochemistry occurs, so both v = 0 and v' = 0 have unit populations. Thus, the summation reduces to the single Franck−Condon term, $S_{00}{}^2$. The 0−0 band for the retPSB chromophore is on the red edge of the absorption band at ∼660 nm or 15150 cm^{-1},[8] about 2450 cm^{-1} from the absorption maximum. The small overlap of the absorption and emission spectra of the purple membrane[87] shows that the 0−0 band is not likely to constitute more than 10% of the area of the absorption band, placing an upper limit of 0.1 on $S_{00}{}^2$. Using this rough estimate, we find that, in weak coupling, t_{ET} >10 × 480 fs ≈ 5 ps. This is consistent with strongly anisotropic absorption by the photointermediate.[11,85]

(3) Borohydride reduction of bR leads to a reduced bR (RbR) with a decrease in the transition dipole moment, from 10.4 to 8.05 D, and a blue shift in the long-wavelength absorption band, from 570 to 354 nm.[14] Despite the modest decrease in the transition moment magnitude, RbR shows no exciton couplet centered at 354 nm. Wu and El-Sayed simulated the CD spectrum of RbR assuming that the exciton splitting and rotational strengths are $^2/_3$ (the approximate ratio of the dipole strengths) those of bR, that the monomer contribution is the same as that of bR, and using the experimental bandwidth of RbR. The simulated spectrum showed an asymmetric negative couplet with a short-wavelength positive lobe about 2.5 times as intense as the long-wavelength negative lobe. This conflicts with the observation of an apparently simple positive CD band at 354 nm in reduced bR.

The couplet strength of an exciton band (eq 1) is proportional to $\mu^4\lambda_0/\Delta^2$, since both R_+ and $\delta\lambda$ are proportional to μ^2. The ratio of transition moments for RbR and bR is 0.774.[14] The ratio of band widths on the wavelength scale, according to Figure 3 of Wu and El-Sayed,[14] is 0.675, and the ratio of wavelengths is 0.628. Therefore,

$$S_{RbR}/S_{bR} = (0.774^4)(0.628)/(0.675^2) = 0.495 \tag{12}$$

The RbR couplet should be only half as strong as that of bR. This would give a couplet strength of ∼ −12.4 for reduced bR, which should be still observable, provided another of Wu and El-Sayed's assumptions is correct—that the intrinsic CD and the coupling contributions are the same for RbR and bR. The reduced chromophore is likely to differ in conformation, and therefore, both its intrinsic rotational strength and its coupling with aromatic and peptide chromophores will differ from those of bR. In fact, a rotational strength of 0.88 DBM, nearly 3 times the net rotational strength of the 570 nm band of bR, is reported[14] for the 358 nm band of RbR.

We simulated the RbR spectrum using the assumptions made by Wu and El-Sayed[14] but using two values for the net rotational strength of the 358 nm band: the value of 0.32 DBM, reported for the 570 nm band of bR,[14] and 0.88 DBM, reported for the 358 nm band of RbR.[14] The results are shown in Figure S4 (Supporting Information). In the former case, as reported by Wu and El-Sayed, the CD spectrum shows a distinct couplet. In the latter case, the positive lobe of the couplet strongly dominates, with an intensity >20 times that of the negative lobe. The CD spectra reported by Wu and El-Sayed for RbR are in fact consistent with this latter simulation: the wavelength maximum in CD is at 354 nm, shifted to the blue with respect to λ_{max} in absorption (358 nm), and close inspection of Wu and El-Sayed's Figure 2 shows a weak negative feature above 400 nm, consistent with our simulation. Thus, RbR appears to exhibit exciton coupling, but this is largely masked by a positive intrinsic rotational strength which is stronger than that observed for bR.

(4) El-Sayed and co-workers[12,14] cited, as evidence against the exciton model, the observation[88] of a CD couplet in the spectra of the L- and M-intermediates, which they argued should either show no exciton effect or a drastically altered effect. El-Sayed et al.[12] state: "In the L_{550} intermediate, one of the three retinal electronic systems has shifted its absorption by >600 cm^{-1} (which is larger than the exciton splitting). This should greatly change the exciton band structure, split the doubly degenerate state, and thus change the relative intensity of the negative and positive loops in their CD spectra." In the experiments to which they refer[89] and other similar experiments,[6,90−92] a large fraction (80% or more) of the bR molecules are obtained in the intermediate form by irradiating at low temperatures. This is evident from the disappearance of

the 570 nm absorption band of the resting form of the protein and its replacement by a shifted absorption band (~545 nm for the L-form and ~400 nm for the M-form). Thus, all three monomers will be in the intermediate form in most of the trimers in the membrane, and exciton interactions comparable to those in the unphotolyzed membrane are expected.

It is clear that the L-intermediate shows a CD couplet and this collapses to a single positive band in film spectra,[88] providing strong evidence of exciton coupling, as discussed above. The CD spectra reported for the M-intermediate have shown substantial variation. We suggest that the highly asymmetric couplet reported by Draheim and Cassim[91] and by Zimanyi et al.[88] is the genuine spectrum of the M-intermediate, and that the other reported spectra[6,90,92] were distorted by photoselection or by the presence of other photointermediates.[91] Draheim and Cassim[91] found that the 450 nm negative band persists in the film spectrum of the M-intermediate, which argues for a distinct electronic transition at this wavelength, perhaps the $n\pi^*$ of the unprotonated Schiff base. However, their results do not exclude an exciton contribution masked by strong positive intrinsic and coupling contributions. Thus, rather than evidence against the exciton model, the CD of the L- and perhaps the M-intermediates provide evidence for the model.

(5) Kataoka et al.[17] have reported that the bR mutant D85N shows a single positive CD band at 575 nm, despite evidence from X-ray diffraction that the mutant forms a crystalline lattice like that of wild-type bR. However, the maximum in the CD spectrum is at 575 nm, whereas the absorption maximum is at 605 nm. The CD spectrum of D85N shows an abrupt return to the baseline near 650 nm, whereas the absorption spectrum[93] returns to the baseline above 700 nm. These two features suggest that D85N has a negative exciton couplet obscured by positive contributions from inherent chirality and coupling.

Karnaukhova et al.[18] reported the CD spectra of six mutant bRs, none of which involved substitution of or by an aromatic residue. They reported that only one of these mutants exhibits a CD couplet similar to that of wild-type bR. Two others show only a weak negative band on the long-wavelength edge of the positive visible band, and the other three show only positive CD in the long-wavelength region. Chemical cross-linking provided evidence that the trimeric structure of bR is preserved in all of the mutants. Karnaukhova et al. interpreted these observations as evidence against the exciton model for bR. However, the three mutants which have apparently simple positive CD bands have a CD maximum at 540 nm and an absorption maximum at 560 nm. This is consistent with an underlying negative couplet and, together with the definite evidence for such a couplet in the other three mutants, suggests that all six mutants have negative exciton couplets of varying magnitudes relative to the positive net rotational strength.

(6) Karnaukhova et al.[16] studied purple membrane reconstituted with retinal (A), a merocyanine analogue of retinal (B), or a mixture of the two. Heterotrimers were formed with one retinal and one merocyanine (ABO, where O denotes a vacant opsin), with one retinal and two merocyanines (ABB), or with two retinals and one merocyanine (AAB). Heterotrimers were also formed with retinal and two other retinal analogues, but most of the reported data were for the A/B heterotrimers. The merocyanine PSB has a long-wavelength absorption band at 662 nm, ε_{max} = 69000 M^{-1} cm^{-1}, a transition dipole moment of 9.2 D, and a bandwidth of 35 nm.[94] Karnaukhova et al. anticipated that nondegenerate exciton coupling between the retinal and merocyanine PSBs would generate a negative band in the 640 nm region, analogous to the negative couplet observed in bR. Instead, they observed positive bands at both 540 and 640 nm for ABO and ABB trimers and a positive 540 nm band but only very weak CD in the 640 nm region for the AAB trimer. Karnaukhova et al. concluded from the absence of the expected negative band that there was no nondegenerate exciton coupling in the heterotrimers and, by extension, no degenerate exciton coupling in the homotrimers AAA and BBB.

However, Karnaukhova et al.[16] did not take into account the significant net positive rotational strengths of the retinal and merocyanine PSBs arising from inherent chirality and coupling with protein groups, as evidenced by the asymmetry of the couplets in the homotrimers. If we neglect the difference in the transition moment magnitudes, μ_i and μ_j, the rotational strength R_{het} due to nondegenerate coupling between chromophores i and j is proportional to R_{exc} due to degenerate coupling among the i chromophores,[81] with a proportionality factor of

$$\frac{4V_{ij}\nu_j}{(\nu_j^2 - \nu_i^2)} \tag{12}$$

where V_{ij} is the Coulombic coupling between the chromophores (eq S38, Supporting Information), and ν_i and ν_j are the frequencies of the transitions i and j. Using $|V_{ij}|$ = 17.7 cm^{-1} for the coupling energy in the trimer and R_{exc} = −39.39 DBM, we calculate R_{het} = −0.441 DBM. This must be corrected by $(\mu_{mc}/\mu_{ret})^2$ = 0.74, where μ_{mc} and μ_{ret} are, respectively, the transition moment magnitudes for the merocyanine and retinal PSBs (both V_{ij} and R_{exc} are proportional to μ_j), giving R_{het} = −0.326 DBM, comparable in magnitude to the net rotational strength of the 570 nm band of the retPSB (Table 1).

Table S8 (Supporting Information) shows the rotational strengths and $\Delta\varepsilon_{max}$ values expected for the 540 and 640 nm bands of the heterotrimers. The observation[16] that in AAB the 640 nm band has almost disappeared implies that $R_{het} \approx -R_{mc}/2$, where R_{mc} is the net rotational strength of the merocyanine PSB. The spectra of AAB and ABB are qualitatively consistent with this analysis, but quantitative analysis is not possible because absolute spectra were not reported.

Another argument that Karnaukhova et al.[16] made against the exciton origin of the 570 nm couplet is that, based upon the X-ray structure,[10] the sign of the couplet should be *positive*, rather than negative. In Figure 7 of their paper, Karnaukhova et al. show a view of two chromophores in the trimer and point out that they are related in a right-handed screw sense. On this basis, they concluded that the exciton couplet should be positive. However, they failed to note that the arrangement of the chromophores is such that their coupling energy is *negative*, as we have shown here. As pointed out by Harada and Nakanishi,[71] it is the *product* of the coupling energy V and the scalar triple product, $\mathbf{R}_{12}\cdot\boldsymbol{\mu}_1\times\boldsymbol{\mu}_2$, that determines the sign of the exciton couplet. A right-handed arrangement of the chromophores means that the scalar triple product is positive. Thus, if $V > 0$, the couplet will be positive. If $V < 0$, as in the present case, the couplet will be negative. In some cases, it may be very difficult to ascertain the sign of both V and the scalar triple product from the simple inspection of a molecular model. In particular, when the angles between the transition moments and the center-to-center direction deviate substantially from 90°, the perspective offered by simple molecular diagrams may

dx.doi.org/10.1021/jp212166k | J. Phys. Chem. B 2012, 116, 6751−6763

be misleading, and the application of the so-called exciton chirality rule should be considered with caution.

CONCLUSIONS

This work demonstrates that exciton coupling among the retPSB chromophores of the purple membrane provides a satisfactory explanation of the CD couplet observed in the 570 nm region. This result is consistently found by explicit quantum-mechanical calculations of retPSB trimers and by exciton and DeVoe calculations on retPSB aggregates of various sizes. A second electronic transition in the 570 nm region is not supported by our results, and there is no experimental evidence for protein heterogeneity. The exciton couplet centered at 570 nm is dominated by intratrimeric exciton couplings. However, both intertrimeric exciton couplings and extrinsic couplings with protein transitions are significant. In fact, intertrimeric exciton couplings reduce the overall intensity of the exciton couplet by a factor of ∼2, while extrinsic couplings are responsible for the nonconservative appearance of the couplet in which the positive short-wavelength branch is definitely more intense than the negative long-wavelength one.

The nearly planar conformation of retPSB in bR makes the intrinsic rotational strength small. This is at odds with rhodopsin, where the strong deviation of the *cis*-PSB chromophore from planarity makes the intrinsic term dominant in determining the visible CD bands.

ASSOCIATED CONTENT

Supporting Information

Detailed methods; additional results; Tables S1−S8; Figures S1−S4; references for Supporting Information. This material is available free of charge via the Internet at http://pubs.acs.org.

AUTHOR INFORMATION

Corresponding Author

*E-mail: ripes@dcci.unipi.it (G.P.); rww@lamar.colostate.edu (R.W.W.).

Notes

The authors declare no competing financial interest.

ACKNOWLEDGMENTS

The authors wish to thank Professors Koji Nakanishi and Nina Berova (Columbia University) and Lorenzo Di Bari (University of Pisa) for useful discussions.

REFERENCES

(1) Becher, B.; Ebrey, T. G. *Biochem. Biophys. Res. Commun.* **1976**, *69*, 1−6.
(2) Cherry, R. J.; Heyn, M. P.; Oesterhelt, D. *FEBS Lett.* **1977**, *78*, 25−30.
(3) Schellman, J. A. *Acc. Chem. Res.* **1968**, *1*, 144−151.
(4) Bayley, P. M. *Prog. Biophys. Mol. Biol.* **1973**, *27*, 1−76.
(5) Becher, B. M.; Cassim, J. Y. *Biophys. J.* **1975**, *15*, A66.
(6) Heyn, M. P.; Bauer, P. J.; Dencher, N. A. *Biochem. Biophys. Res. Commun.* **1975**, *67*, 897−903.
(7) Muccio, D. D.; Cassim, J. Y. *Biophys. J.* **1979**, *26*, 427−440.
(8) Ebrey, T. G.; Becher, B.; Mao, B.; Kilbride, P.; Honig, B. *J. Mol. Biol.* **1977**, *112*, 377−397.
(9) Kriebel, A. N.; Albrecht, A. C. *J. Chem. Phys.* **1976**, *65*, 4575−4583.
(10) Luecke, H.; Schobert, B.; Richter, H.-T.; Cartailler, J.-P.; Lanyi, J. K. *J. Mol. Biol.* **1999**, *291*, 899−911.
(11) El Sayed, M. A.; Karvaly, B.; Fukumoto, J. M. *Proc. Natl. Acad. Sci. U.S.A.* **1981**, *78*, 7512−7516.
(12) El Sayed, M. A.; Lin, C. T.; Mason, W. R. *Proc. Natl. Acad. Sci. U.S.A.* **1989**, *86*, 5376−5379.
(13) Jang, D. J.; El Sayed, M. A.; Stern, L. J.; Mogi, T.; Khorana, H. G. *FEBS Lett.* **1990**, *262*, 155−158.
(14) Wu, S. G.; El Sayed, M. A. *Biophys. J.* **1991**, *60*, 190−197.
(15) Cassim, J. Y. *Biophys. J.* **1992**, *63*, 1432−1442.
(16) Karnaukhova, E.; Vasileiou, C.; Wang, A.; Berova, N.; Nakanishi, K.; Borhan, B. *Chirality* **2006**, *18*, 72−83.
(17) Kataoka, M.; Mihara, K.; Kamikubo, H.; Needleman, R.; Lanyi, J. K.; Tokunaga, F. *FEBS Lett.* **1993**, *333*, 111−113.
(18) Karnaukhova, E.; Schey, K. L.; Crouch, R. K. *Amino Acids* **2006**, *30*, 17−23.
(19) Takeda, K.; Sato, H.; Hino, T.; Kono, M.; Fukuda, K.; Sakurai, I.; Okada, T.; Kouyama, T. *J. Mol. Biol.* **1998**, *283*, 463−474.
(20) Pescitelli, G.; Kurtán, T.; Flörke, U.; Krohn, K. *Chirality* **2009**, *21*, E181−E201.
(21) Pescitelli, G.; Sreerama, N.; Salvadori, P.; Nakanishi, K.; Berova, N.; Woody, R. W. *J. Am. Chem. Soc.* **2008**, *130*, 6170−6181.
(22) *Spartan'08*; Wavefunction, Inc.: Irvine, CA.
(23) Dreuw, A.; Head-Gordon, M. *Chem. Rev.* **2005**, *105*, 4009−4037.
(24) Elliott, P.; Furche, F.; Burke, K. Excited States from Time-Dependent Density Functional Theory. In *Rev. Comput. Chem.*; Lipkowitz, K. B., Cundari, T. R., Eds.; John Wiley & Sons, Inc.: Hoboken, NJ, 2009; Vol. *26*, pp 91−165.
(25) Jacquemin, D.; Wathelet, V.; Perpete, E. A.; Adamo, C. *J. Chem. Theory Comput.* **2009**, *5*, 2420−2435.
(26) Autschbach, J.; Nitsch-Velasquez, L.; Rudolph, M. *Top. Curr. Chem.* **2011**, *298*, 1−98.
(27) Ridley, J.; Zerner, M. *Theor. Chim. Acta* **1973**, *32*, 111−134.
(28) Ridley, J. E.; Zerner, M. C. *J. Mol. Spectrosc.* **1974**, *50*, 457−473.
(29) Frisch, M. J.; Trucks, G. W.; Schlegel, H. B.; Scuseria, G. E.; Robb, M. A.; Cheeseman, J. R.; Scalmani, G.; Barone, V.; Mennucci, B.; Petersson, G. A.; et al. *Gaussian 09*, revision A.02; Gaussian, Inc.: Wallingford, CT, 2009.
(30) Becke, A. D. *J. Chem. Phys.* **1993**, *98*, 5648−5652.
(31) Becke, A. D. *Phys. Rev. A* **1988**, *38*, 3098−3100.
(32) Becke, A. D. *J. Chem. Phys.* **1993**, *98*, 1372−1377.
(33) Adamo, C.; Barone, V. *J. Chem. Phys.* **1999**, *110*, 6158−6170.
(34) Yanai, T.; Tew, D. P.; Handy, N. C. *Chem. Phys. Lett.* **2004**, *393*, 51−57.
(35) Schäfer, A.; Huber, C.; Ahlrichs, R. *J. Chem. Phys.* **1994**, *100*, 5829−5835.
(36) Ansgar, S.; Hans, H.; Reinhart, A. *J. Chem. Phys.* **1992**, *97*, 2571−2577.
(37) Kendall, R. A.; Dunning, J. T. H.; Harrison, R. J. *J. Chem. Phys.* **1992**, *96*, 6796−6806.
(38) Bruhn, T.; Hemberger, Y.; Schaumlöffel, A.; Bringmann, G. *Specdis v. 1.51*; University of Würzburg: Würzburg, Germany, 2011.
(39) DeVoe, H. *J. Chem. Phys.* **1964**, *41*, 393−400.
(40) DeVoe, H. *J. Chem. Phys.* **1965**, *43*, 3199−3208.
(41) Cech, C. L.; Hug, W.; Tinoco, I. Jr. *Biopolymers* **1976**, *15*, 131−152.
(42) Woody, R. W. *J. Am. Chem. Soc.* **2009**, *131*, 8234−8245.
(43) Woody, R. W.; Sreerama, N. *J. Chem. Phys.* **1999**, *111*, 2844−2845.
(44) Oesterhelt, D.; Hess, B. *Eur. J. Biochem.* **1973**, *37*, 316−326.
(45) Hasselbacher, C. A.; Spudich, J. L.; Dewey, T. G. *Biochemistry* **1988**, *27*, 2540−2546.
(46) Kollbach, G.; Steinmuller, S.; Berndsen, T.; Buss, V.; Gartner, W. *Biochemistry* **1998**, *37*, 8227−8232.
(47) Wanko, M.; Hoffmann, M.; Frauenheim, T.; Elstner, M. *J. Comput.-Aided Mol. Des.* **2006**, *20*, 511−518.
(48) Aquino, A. J. A.; Barbatti, M.; Lischka, H. *ChemPhysChem* **2006**, *7*, 2089−2096.
(49) Iyama, T.; Kawabata, H.; Tachikawa, H. *Synth. React. Inorg., Met.-Org., Nano-Met. Chem.* **2010**, *40*, 306−311.
(50) Savedra, R. M. L.; Pinto, M. F. S.; Trsic, M. *J. Chem. Phys.* **2006**, *125*, 144901/1−144901/7.

(51) Send, R.; Sundholm, D. *Phys. Chem. Chem. Phys.* **2007**, *9*, 2862−2867.
(52) Send, R.; Sundholm, D. *J. Phys. Chem. A* **2007**, *111*, 27−33.
(53) Silva López, C.; Nieto Faza, O.; López Estévez, S.; De Lera, A. R. *J. Comput. Chem.* **2006**, *27*, 116−123.
(54) Fujimoto, K.; Hayashi, S.; Hasegawa, J.-y.; Nakatsuji, H. *J. Chem. Theory Comput.* **2007**, *3*, 605−618.
(55) Sun, M.; Ding, Y.; Cui, G.; Liu, Y. *J. Phys. Chem. A* **2007**, *111*, 2946−2950.
(56) Wanko, M.; Garavelli, M.; Bernardi, F.; Niehaus, T. A.; Frauenheim, T.; Elstner, M. *J. Chem. Phys.* **2004**, *120*, 1674−1692.
(57) Wanko, M.; Hoffmann, M.; Strodel, P.; Koslowski, A.; Thiel, W.; Neese, F.; Frauenheim, T.; Elstner, M. *J. Phys. Chem. B* **2005**, *109*, 3606−3615.
(58) Guido, C. A.; Jacquemin, D.; Adamo, C.; Mennucci, B. *J. Phys. Chem. A* **2010**, *114*, 13402−13410.
(59) Rostov, I. V.; Amos, R. D.; Kobayashi, R.; Scalmani, G.; Frisch, M. J. *J. Phys. Chem. B* **2010**, *114*, 5547−5555.
(60) Send, R.; Sundholm, D.; Johansson, M. P.; Pawłowski, F. *J. Chem. Theory Comput.* **2009**, *5*, 2401−2414.
(61) Grimme, S.; Furche, F.; Ahlrichs, R. *Chem. Phys. Lett.* **2002**, *361*, 321−328.
(62) Altun, A.; Yokoyama, S.; Morokuma, K. *J. Phys. Chem. B* **2008**, *112*, 6814−6827.
(63) Andruniów, T.; Ferré, N.; Olivucci, M. *Proc. Natl. Acad. Sci.* **2004**, *101*, 17908−17913.
(64) Vreven, T.; Morokuma, K. *Theor. Chim. Acta* **2003**, *109*, 125−132.
(65) Mathies, R.; Stryer, L. *Proc. Natl. Acad. Sci. U.S.A.* **1976**, *73*, 2169−2173.
(66) Cembran, A.; Gonzalez-Luque, R.; Altoe, P.; Merchan, M.; Bernardi, F.; Olivucci, M.; Garavelli, M. *J. Phys. Chem. A* **2005**, *109*, 6597−6605.
(67) Heyn, M. P.; Cherry, R. J.; Muller, U. *J. Mol. Biol.* **1977**, *117*, 607−620.
(68) Bogomolni, R. A.; Hwang, S. B.; Tseng, Y. W.; King, G. I.; Stoeckenius, W. *Biophys. J.* **1977**, *17*, A98.
(69) King, G. I.; Mowery, P. C.; Stoeckenius, W.; Crespi, H. L.; Schoenborn, B. P. *Proc. Natl. Acad. Sci. U.S.A.* **1980**, *77*, 4726−4730.
(70) Tachikawa, H.; Kawabata, H. *J. Photochem. Photobiol., B* **2005**, *79*, 191−195.
(71) Harada, N.; Nakanishi, K. *Circular Dichroic Spectroscopy - Exciton Coupling in Organic Stereochemistry*; University Science Books: Mill Valley, CA, 1983.
(72) Superchi, S.; Giorgio, E.; Rosini, C. *Chirality* **2004**, *16*, 422−451.
(73) Woody, R. W. *Chirality* **2005**, *17*, 450−455.
(74) Ito, H. *Trends Chem. Phys.* **2000**, *8*, 75−130.
(75) Cicchi, S.; Ghini, G.; Lascialfari, L.; Brandi, A.; Betti, F.; Berti, D.; Baglioni, P.; Di Bari, L.; Pescitelli, G.; Mannini, M.; Caneschi, A. *Soft Matter* **2010**, *6*, 1655−1661.
(76) Cicchi, S.; Pescitelli, G.; Lascialfari, L.; Ghini, G.; Di Bari, L.; Brandi, A.; Bussotti, L.; Atsbeha, T.; Marcelli, A.; Foggi, P.; Mannini, M. *Chirality* **2011**, *23*, 833−840.
(77) Simpson, W. T.; Peterson, D. L. *J. Chem. Phys.* **1957**, *26*, 588−593.
(78) Pescitelli, G.; Gabriel, S.; Wang, Y.; Fleischhauer, J.; Woody, R. W.; Berova, N. *J. Am. Chem. Soc.* **2003**, *125*, 7613−7628.
(79) Okada, T.; Sugihara, M.; Bondar, A. N.; Elstner, M.; Entel, P.; Buss, V. *J. Mol. Biol.* **2004**, *342*, 571−583.
(80) Bauer, P. J.; Dencher, N. A.; Heyn, M. P. *Biophys. Struct. Mech.* **1976**, *2*, 79−92.
(81) Tinoco, I. Jr. *Adv. Chem. Phys.* **1962**, *4*, 113−160.
(82) Wellman, K. M.; Laur, P. H. A.; Briggs, W. S.; Moscowitz, A.; Djerassi, C. *J. Am. Chem. Soc.* **1965**, *87*, 66−72.
(83) Dobler, J.; Zinth, W.; Kaiser, W.; Oesterhelt, D. *Chem. Phys. Lett.* **1988**, *144*, 215−220.
(84) van den Berg, R.; Jang, D. J.; Bitting, H. C.; El-Sayed, M. A. *Biophys. J.* **1990**, *58*, 135−141.
(85) Godfrey, R. E. *Biophys. J.* **1982**, *38*, 1−6.
(86) Kasha, M. *Radiat. Res.* **1963**, *20*, 55−70.
(87) Lewis, A.; Spoonhower, J. P.; Perreault, G. J. *Nature* **1976**, *260*, 675−678.
(88) Zimanyi, L.; Tokaji, Z.; Dollinger, G. *Biophys. J.* **1987**, *51*, 145−148.
(89) Zimanyi, L.; Tokaji, Z.; Dollinger, G. *Acta Physiol. Hung.* **1988**, *71*, 158.
(90) Yoshida, M.; Ohno, K.; Takeuchi, Y.; Kagawa, Y. *Biochem. Biophys. Res. Commun.* **1977**, *75*, 1111−1116.
(91) Draheim, J. E.; Cassim, J. Y. *Biophys. J.* **1985**, *47*, 497−507.
(92) Steinmuller, S.; Buss, V.; Gartner, W. *J. Photochem. Photobiol., B* **1995**, *31*, 139−144.
(93) Turner, G. J.; Miercke, L. J. W.; Thorgeirsson, T. E.; Kliger, D. S.; Betlach, M. C.; Stroud, R. M. *Biochemistry* **1993**, *32*, 1332−1337.
(94) Derguini, F.; Caldwell, C. G.; Motto, M. G.; Balogh-Nair, V.; Nakanishi, K. *J. Am. Chem. Soc.* **1983**, *105*, 646−648.
(95) Becher, B.; Cassim, J. Y. *Biophys. J.* **1976**, *16*, 1183−1200.
(96) Brown, A.; Kemp, C. M.; Mason, S. F. *J. Chem. Soc. A* **1971**, 751−755.